Preprints, 10th Conference on Manoeuvring and Control of Marine Craft
August 24-26, 2015. Copenhagen, Denmark

Development of USV Autonomy for the 2014 Maritime RobotX Challenge

Minju Kang[1], Sungchur Kwon[1], Jeonghong Park[1], Taeyun Kim[1], Jungwook Han[1], Jeonghyeon Wang[2], Seonghun Hong[2], Yeonjoo Shim[1], Sukmin Yoon[1], Byunghyun Yoo[1], and Jinwhan Kim[1,2*]

[1] *Department of Mechanical Engineering, Korea Advanced Institute of Science and Technology, Daejeon, Korea (e-mail: jinwhan@kaist.ac.kr)*
[2] *Robotics Program, Korea Advanced Institute of Science and Technology, Daejeon, Korea*

Abstract: The inaugural Maritime RobotX Challenge competition was held in Marina Bay, Singapore between October 20-26 in 2014. The competition composed of five mission tasks in which intelligence is the single most important factor, and all the mission tasks were required to be performed autonomously with no human intervention. We participated in the competition as the KAIST team with our own unmanned surface vehicle integrated with various sensors for autonomous navigation and perception. All the software algorithms for vehicle autonomy including mission management, environmental perception, path planning and control were developed and applied in the actual competition. This paper describes the given mission tasks of the competition and how the vehicle intelligence and control algorithms were designed in order to perform those mission tasks autonomously.

Keywords: Unmanned surface vehicle, vehicle autonomy, navigation, perception

1. INTRODUCTION

Recently, unmanned vehicle systems technology has been greatly improved with the advance of computer capabilities and artificial intelligence. Among various types of unmanned vehicle systems, unmanned surface vehicles (USVs), also known as unmanned surface vessels, have attracted much interest for their ability to perform various missions in marine environments such as environmental monitoring, hydrographic survey, coastal security, search-and-rescue, etc.

In line with this, the inaugural Maritime RobotX Challenge (http://www.robotx.org) was held in Marina Bay, Singapore between October 20-26, 2014, organized by AUVSI Foundation and sponsored by US office of Naval Research (ONR). The competition was composed of five mission tasks which are closely related to practical applications for USVs. Intelligence is a key factor and all the mission tasks were required to be performed autonomously with no human intervention. The five mission tasks are summarized in the following:

Task 1 - Navigation and control: The boat should traverse a linear course bounded by two sets of gate buoys with different colors (red on the port side and green on the starboard side) at the start and end points whose position coordinates are not provided.

Task 2 - Underwater search and report: The boat should find and report the location (position and depth) of an acoustic sound source (i.e., pinger) in a search area. The pinger is hidden underwater and periodically emits acoustic signals at a frequency between 25∼40 kHz.

Task 3 - Symbol identification and docking: The boat must identify symbols on a placard and enter the designated docking bay. Three marker symbols are circle, triangle, and cruciform, which are placed on each docking bay whose arrangement is not provided in advance.

Task 4 - Buoy observation and report: A light buoy is placed somewhere in a search area and the buoy emits light signals with three different colors (red, green, and blue) in a randomly arranged sequence. The boat should find the location of the buoy and report the correct color sequence.

Task 5 - Obstacle detection and avoidance: The boat should enter the course through a designated entry gate, navigate the course area filled with different sizes of obstacle buoys without collision (or contact), and complete the course by passing through a designated exit gate.

We developed a 4m-long USV system to participate in the competition using a 16-foot long catamaran hull platform (i.e., WAM-V by Marine Advanced Research). The specifications and configurations of the electronics and propulsion systems were designed and integrated using commercial-off-the-shelf (COTS) components. In particular, various sensors were installed on the USV for autonomous navigation and perception. To be more specific, an integrated IMU/GPS system was used for navigation. A camera and a lidar were for environmental perception and a hydrophone array for the underwater search task. Then, the computer algorithms for fusing the measure-

ments from the above-mentioned sensors were developed considering the given mission requirements. The computer codes were implemented in C/C++ for real-time operation and hardware/software interface towards the developed USV system. The performance of the algorithms were demonstrated with experimental tests and eventually at the on-site competition.

2. USV DESIGN AND DEVELOPMENT

2.1 USV platform system

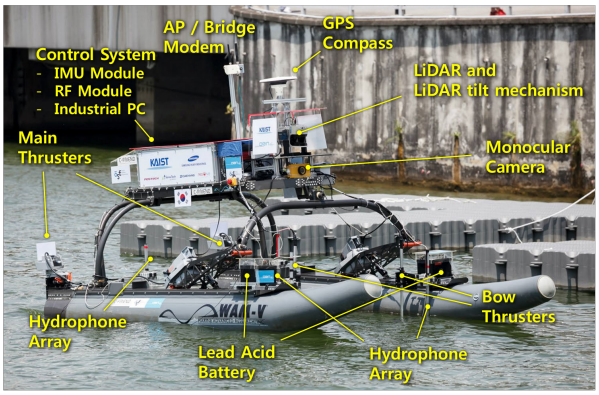

Fig. 1. KAIST USV system

In order to perform the given mission tasks, the USV required the capability of perceiving the surrounding surface-water and underwater environments. For navigation, the USV was equipped with an integrated GPS/IMU system to estimate the pose of the USV. Specifically, a GPS compass and a MEMS IMU were used. In addition to navigation sensors, the USV system was equipped with a monocular camera, two lidars and hydrophone arrays for exteroceptive sensing. The monocular camera and the lidars were mounted to the front of the main deck plate and used to detect and identify various features and structures on the water surface. The camera with a wide lens has a field of view angle of 110°, and the frame rate is 10 fps. The SICK lidar has a planar sweep of 190°and its sampling rate to acquire measurements is 10 Hz. A nodding mechanism was implemented using a step motor that can tilt the lidar up and down at approximately 0.8 Hz from 20°to -20°for three-dimensional scanning of the surrounding environment. To find the location of a sound source, four hydrophones were installed on the lower hull of the USV, two on the starboard side and two on the port.

Two industrial PCs were used for autonomous perception, navigation and control. The primary PC dealt with control, navigation, underwater acoustics, and task management, and the secondary PC took charge of processing camera and lidar measurement. These two PCs are connected via a TCP/IP communication link. Work allocation between two PCs and various algorithm modules is shown in Fig. 2.

For mobility, two electric outboard thrusters were installed on the USV as a main propulsion system considering that the boat has a catamaran hull form. The USV was designed to be steered using differential thrust in nominal operating conditions. In addition, two outboard thrusters

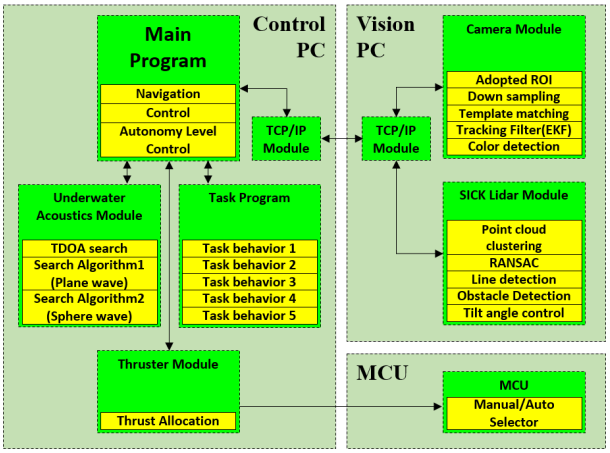

Fig. 2. Software structure of KAIST USV

are installed in the fore part of the twin hull to achieve station-keeping and parallel maneuvering capabilities. All the onboard systems of the USV including the propulsion system were electrically powered by batteries. The duration was expected to be over 6 hours, slightly varying with operating conditions.

2.2 Navigation, guidance and control

The Kalman filter algorithm was applied to the navigation filter. Three degree-of-freedom (DOF) motion composed of surge, sway, and yaw was considered for the filter dynamics. The USV's motion was estimated using position and attitude measurements provided by the the GPS-compass and IMU. The state vector to represent this 3-DOF motion can be expressed as

$$\mathbf{x} = \begin{bmatrix} x & y & \psi & u & v & \dot{\psi} \end{bmatrix} \tag{1}$$

where x, y and ψ represent the position and heading of the USV in the global reference frame. u and v are the USV's velocity in the body-fixed frame. The USV was able to localize itself and navigate the course area reliably with the 3-DOF based GPS-IMU integrated navigation system.

In fact, accurate sensor measurement such as lidar's point cloud data is important to carry out mission tasks. Because the lidar provides the point cloud data in the body-fixed frame, it is required to compensate roll and pitch motions of the USV from the sensor measurement. For this reason, these extra states were additionally measured using IMU.

For guidance and control, three maneuvering modes(course tracking, weathervaning, position keeping) were defined and different control strategies were designed and applied as decribed in the following.

Waypoint tracking: Waypoint tracking was an essential maneuvering capability for every mission task. Waypoints were predefind according to the course information or generated by the boat's planner. The waypoint tracking guidance was applied to minimize line of sight error and cross-track error (Fossen et al. (2003)). The control forces minimizing these errors were determined in the direction of surge and yaw, and control forces were achieved by operating two main thrusters of the USV. The USV was operated efficiently over a wide range of speed in this mode, however its sway motion could not be controlled due to the vehicle's underactuated properties in this mode.

Position keeping: In the position keeping mode, in addition to the main thrusters, two bow thrusters were also used to control the USV motion in position and orientation simultaneously. This enabled the boat to maintain the current pose (i.e., position and orientation) and/or track a sequence of pose commands. This capability was particularly useful for the underwater search and docking mission tasks.

Weathervanning: Weathervanning control was used in the buoy observation mission. The main purpose of weathervanning control was to maintain an appropriate separation between the boat and the light buoy while facing toward the buoy within the camera's field of view. However, the vehicle's heading was not actively controlled in order to avoid fighting against environmental disturbances.

The thrust allocation problem was simplified to a linear-unconstrained optimization problem, so control allocation was achieved by simple matrix calculation. When determining control forces, general PD control law was adopted to minimize target errors throughout the three maneuvering modes.

3. MISSION STRATEGIES AND ALGORITHMS

The competition goal was to accomplish the five mission tasks autonomously. No interaction with the USV was permitted once the USV started the run. Therefore, the mission planner was designed to be able to deal with any unexpected situations adaptively while trying to perform all of the five mission tasks consecutively. The strategies and algorithms for all of the five mission task were designed considering the mission requirements and the USV's sensing capability, which are described in the following.

3.1 Task 1: Navigation and control

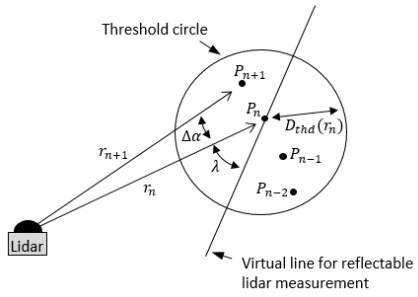

Fig. 3. A diagram to describe scanned lidar data and the ABD approach. The black dots show reflected point cloud and the virtual line is an auxiliary line representing the worst case in which a lidar measurement can be obtained.

The main strategy for the first mission was to traverse the course between the gates by generating four waypoints and performing waypoint tracking control. In order to find the gate buoys, a nodding lidar system was used to collect point cloud data at the start point and candidate point clouds were selected within the predefined region-of-interest (ROI) of the lidar. For the point cloud segmentation in the given lidar data, a 2D segmentation approach which is known as the point-distance-based segmentation (PDBS) algorithm was applied in Premebida and Nunes (2005).

A segment was assigned by finding a break point where the condition $D(r_n, r_{n+1}) > D_{thd}$ is satisfied. The D_{thd} is the threshold condition and $D(r_n, r_{n+1})$ is the Euclidean distance between two consecutive scanned points, as shown in Fig. 3. In this study, the threshold condition called Adaptive Breakpoint Detector (ABD) was used. See Borges and Aldon (2004).

$$D_{thd} = r_n \cdot \frac{\sin(\Delta\alpha)}{\sin(\lambda - \Delta\alpha)} + 3\sigma_r \tag{2}$$

Here, r_n is the range of n_{th} point, λ is the auxiliary parameter and $\Delta\alpha$ is the angle difference between two consecutive scanned points. The σ_r is the residual variance to consider lidar measurement noise.

3.2 Task 2: Underwater search and report

In order to determine the position and depth of the underwater acoustic pinger, the USV was equipped with a hydrophone array system consisting of four hydrophones and amplifiers. The direction to the pinger from the USVs position was computed using the TDOA estimates, and the multilateralization technique was used to determine the location of the pinger. The sound source localization algorithm is composed of two-step approaches. In the first step, it is assumed that the sound source is distant from the boat and the water is relatively shallow. Thus, acoustic waves can be regarded to be unidirectional plane waves in the horizontal plane and the distance from the USV to the sound source can be assumed to be much larger than the array aperture. This allows estimating the pinger's position with a smaller number of hydrophones. After identifying the approximate X-Y position, the USV is maneuvered to approach the sound source and conducts the second step. The second method, which is based on the spherical wave model is applied to find the 3D position of the pinger. Instead of solving nonlinear equation intersecting hyperboloid of each TDOA, a linear closed-form, analytic approach was employed for computational efficiency. For details, see Mahajan and Walworth (2001).

3.3 Task 3: Identify symbol and dock

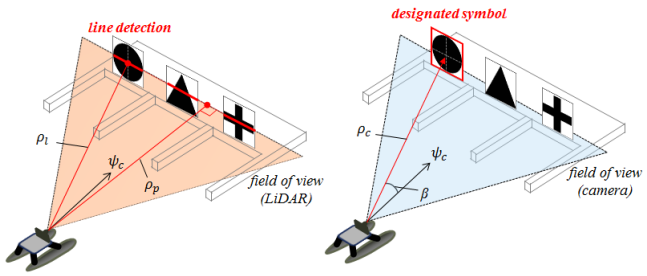

(a) FOV of lidar (b) FOV of camera

Fig. 4. The procedure of maneuvering into the designated docking bay: (a) Detecting the placards on the dock using poing cloud segmentation and line detection from lidar measurement, (b) Identifying symbols by the adpative template matching techiques fusing camera and lidar measurements.

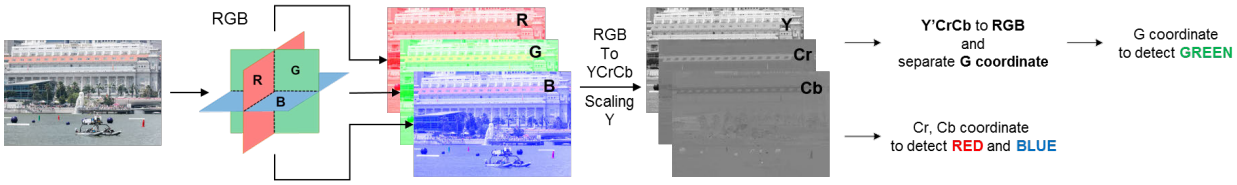

Fig. 5. The procedure of image processing to reduce the effect of the environmental condition. Blue and red is decided in YCrCb color space, and green is detected in RGB color space after scaling Y factor.

In order to enter the correct bay, the vehicle was required to identify a target symbol on a placard using computer vision, which is either a black cruciform or a black triangle or a black circle. Point cloud segmentation and adaptive template matching techniques were employed by fusing lidar and camera measurements. The lidar obtained the point clouds reflected from the placard and the distance to the placards was estimated, as illustrated in Fig. 4(a). In order to find the line of the symbols using the lidar, the PDBS algorithm was applied as described in Task 1, and a line detection algorithm was applied to each segmented point cloud using random sample consensus (RANSAC) technique. Then, relative pose between the boat and placards were acquired. Online image processing algorithms were applied to recognize the symbol and track the relative bearing to the symbol using the adaptive template matching and Extended Kalman Filter (EKF) techniques. Details are described in Brunelli (2008) and Arulampalam (2004). For this process, a down-sampled image was used and the region of interest (ROI) on the image is assigned to improve computational efficiency. The size of the predefined template image and the ROI were adaptively changed by considering the lidars range information from the USV to the detected symbol placard. In addition, the template matching algorithm was used to recognize the designated symbol. After the boat finally decided where to move, sway motion can be applied by using both all of the main and bow thrusters.

3.4 Task 4: Observe and report

In this task, the USV was first required to find the position of the light buoy which was in a randomly placed in the course area. The lidar system was used to find the light buoy. Once the light tower was found, the boat maintained its relative pose by weathervanning control towards the light buoy using lidar measurements. Then, color detection algorithm was applied to determine the color sequence using the computer vision system. The data from the lidar was transformed into the pixel coordinates to determine the position and size of the ROI in pixel coordinates (Zhang and Pless (2004)). After obtaining the ROI of the color panel, the intensity values of the pixel coordinates were averaged to make thresholds for color detection. In our approach, YCrCb color space was applied to overcome the light-disturbance issue (Ahirwal et al. (2007)). In YCrCb color space, Y is the luminance component and Cr and Cb are the red-difference and blue-difference chroma components. Using the Cr and Cb components with certain threshold values, we could distinguish red and blue colors of the LED panel. To separate the green color, Y values were set to zero and converted back to the RGB color space. Then, the green color space could be obtained with little luminance component. Without separating the luminance component, it was difficult to distinguish the background image from LED panel emitting green color, since the green color space was sensitive to the intensity of light. Figure 5 shows the procedure of reducing the effect of lights. After detecting the color of the light buoy, a decision tree was applied to find a color sequence based on the relative intensity change of the pixels in the ROI. Finally, a voting algorithm was used to make a decision for the most likely color sequence. The selected sequence was then reported to judge via TCP/IP communication.

3.5 Task 5: Detect and avoid obstacles

The method for recognizing the gate buoys is similar to the methods described in Task 1. However, the algorithm was extended to deal with the increased number of buoys at each gate, four instead of two in Task 1. Thus, a RANSAC-based line fitting criterion was added to the gate search algorithm. After identifying which gate was the designated entrance, a set of waypoints were generated for the boat to track. Then, the vehicle navigated the course toward the exit gate, and the path planning algorithm was applied to avoid obstacles while navigating the obstacle field. For path planning and obstacle avoidance, the A* algorithm was used as a path planner (Hart et al. (1968) and Garau et al. (2005)), which is known to be the optimal planner in discrete deterministic state-environment settings. The path planner searches for a shortest distance path between the start and goal points without colliding to any of the obstacles. In this procedure, 3D point cloud data provided by lidar were clustered, and the obtained size and relative pose information were delivered from the vision module to the task module. Then, the task module projected the objects into a quantized manhattan grid map with 1m by 1m grid size. However, the obstacle map was not given a priori and the detection process involved measurement errors and uncertainties, which required online replanning capability for the motion planner. Thus, the obstacle map was kept being updated whenever the USV detected a new obstacle in the field of view. The path was continuously replanned based on the updated obstacle map to deal with erroneous sensor measurements and environmental uncertainties.

4. TESTING AND TRIAL PERFORMANCE

For Task 1, the developed approach for gate detection and waypoint tracking control showed satisfactory performance during test runs and the final competition. Figure 6 shows a picture taken during the competition.

For the underwater search mission, collected data are shown in Fig. 7 which are the voltage level changes from the installed hydrophone array system. The signals were

Fig. 6. A captured image for Task 1 during the competition

processed with series of analog bandpass filters. The filter was designed to make measurement voltage decrease from 2.5 V to 0 V when an acoustic signal was detected. The time difference of arrival can be defined as the time interval between the points where the voltage is sharply reduced. Example results from test trials are shown in Fig. 8.

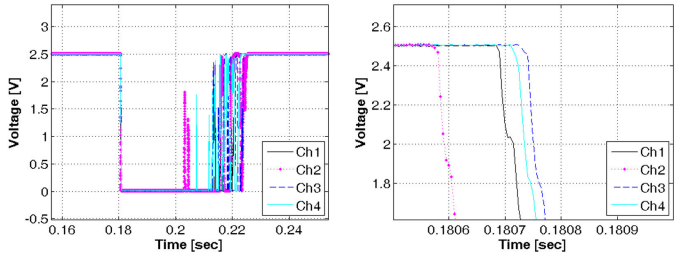

Fig. 7. Hydrophone measurement for the underwater search task

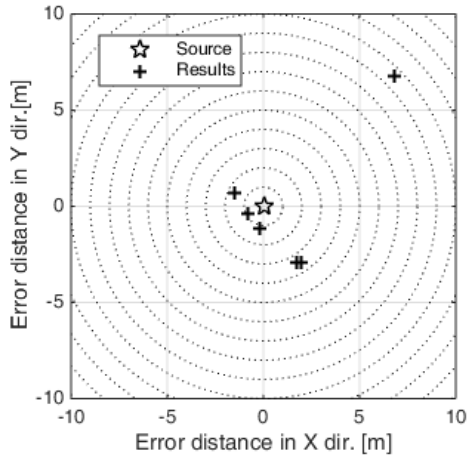

Fig. 8. Sound source localization from test trials

Figure 9 shows the results of identifying the designated symbol and docking performance. In Fig. 9(a), the red lines represent the detected lines of the symbol placards using lidar measurements and the circled line with white dots among them is the symbol representing the designated bay. Note that only two symbol placards were installed in the experiment in Fig. 9(b). After the line detection of symbol placards is done, the results of the subsequent proposed algorithm is shown in Fig. 9(b). The green box represents the symbol region estimated by EKF and the cyan dot represents the center of the selected symbol computed through template matching. The real-time docking performance can be found in Fig. 9(c).

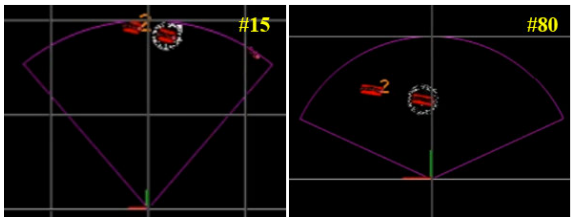

(a)

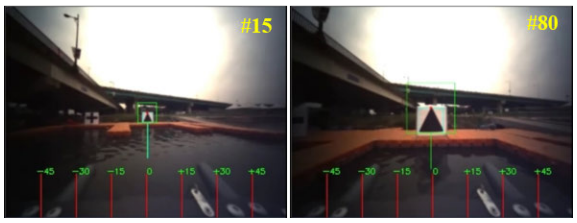

(b)

Fig. 9. Experimental results of the docking mission: (a) Placard detection using lidar measurements; (b) Symbol identification and relative position detection of the symbol by the tracking filter.

Figure 10 shows the results of LED panel detection with the image ROI and relative color changes in three color coordinates respectively. As Fig. 10(a) shows, the color can be either blue or green or red. Figure 10 (b) plots the color changes in each frame which implies that it is desirable to detect only one color at a time. In Fig. 10(b), the color difference in Cb which is the coordinate to detect blue color suddenly increases near the 40th frame, the green coordinate suddenly increases near the 45th frame and the Cr coordinate increases near the 50th frame. Using the decision tree algorithm, these color changes are classified as a sequence of blue-green-red.

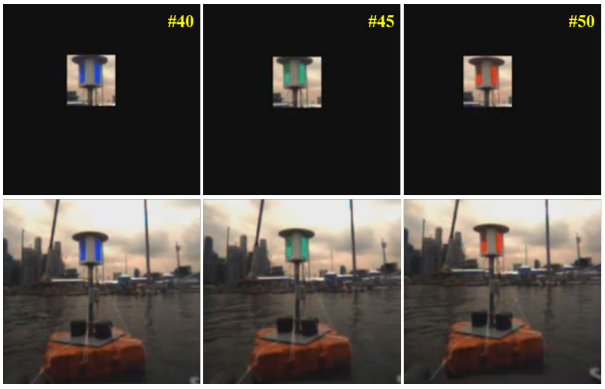

(a) Camera view of the light buoy and ROI extraction

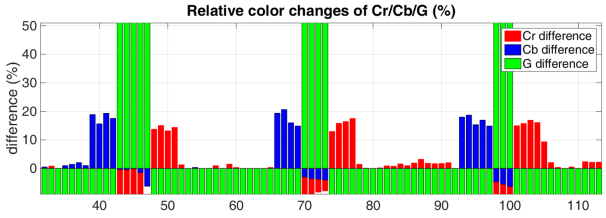

(b) Relative color changes of the LED panels

Fig. 10. Results of the light buoy detection and relative color differences of each coordinate: (a) illustrates the light buoy and the ROI obtained from the calibrated lidar data; (b) depicts the relative color changes of the LED panel after image processing.

For Task 5, two different approaches were prepared in advance to cope with the uncertainty of the competition site. One was to use an infrared light based lidar (i.e., Leddar sensor from LeddarTech) and the other one was to use a nodding lidar system (i.e., SICK lidar). Each approach has its pros and cons in the field of view (FOV), vertical beam coverage and sampling time. The comparison is given in Fig. 11.

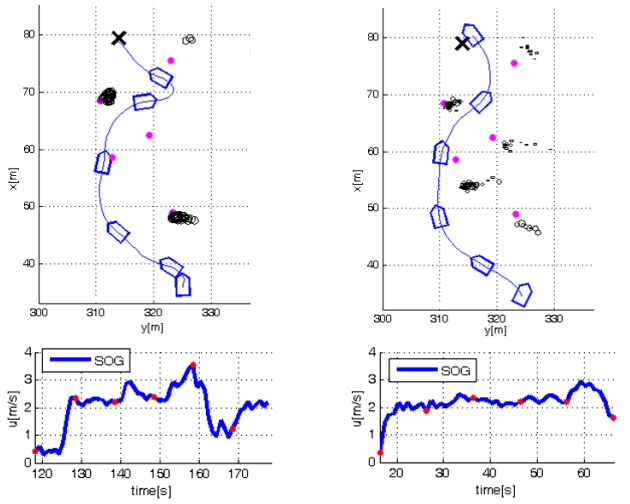

(a) A* with Leddar (b) A* with SICK lidar

Fig. 11. Comparison between detecting sensors and avoiding algorithms

The lidar system was chosen for the final competition, to get a wider FOV and deal with densely arranged obstacles. The real situation is described in Fig. 12. The produced 3D point clouds are projected to the vehicle's motion plane considering the nature of surface vehicle operation.

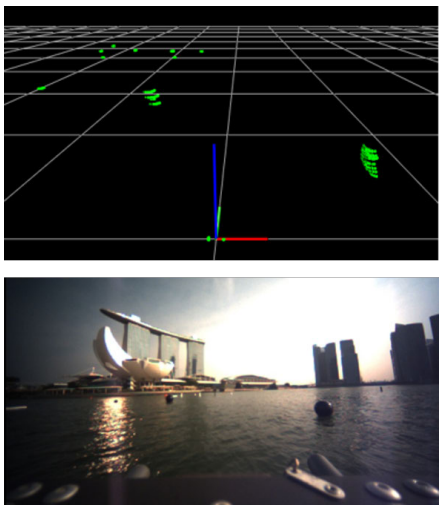

Fig. 12. Obstacle detection during the competition

5. CONCLUSION

This paper addressed the development procedures of the USV system focusing on vehicle autonomy and our team strategies for the 2014 Maritime RobotX challenge competition. The competition was held in a real sea environment with changing weather conditions. Therefore, the system's reliability was a key consideration throughout the design and development phases. The teams conducted a number of outdoor tests for performance validation, which made it possible for our team to successfully complete the actual competition. Our future work will focus on further improving the vehicle's autonomy for more practical and realistic USV applications.

ACKNOWLEDGMENTS

We would like to appreciate the generous support from the competition sponsors for giving us the resources and the opportunity to work on this competition. We greatly thank Samsung Heavy Industries and KAIST for their financial support, and SonarTech Inc., Redone technologies, Deayang Electric, and LeddarTech for their equipment and technical support. We would also like to thank Prof. Huynchul Shim and Prof. Hyun Myung at KAIST and Prof. Son-Cheol Yu at POSTECH for their advice and help as our joint team members.

REFERENCES

Ahirwal, B., Khadtare, M., and Mehta, R. (2007). Fpga based system for color space transformation rgb to yiq and ycbcr. In *Intelligent and Advanced Systems, 2007. ICIAS 2007. International Conference on*, 1345–1349. IEEE.

Arulampalam, B.R.S. (2004). *Beyond the Kalman filter: Particle filters for tracking applications*. Artech House.

Borges, G.A. and Aldon, M.J. (2004). Line extraction in 2d range images for mobile robotics. *Journal of Intelligent and Robotic Systems*, 40(3), 267–297.

Brunelli, R. (2008). *Template matching techniques in computer vision*. Wiley.

Fossen, T.I., Breivik, M., and Skjetne, R. (2003). Line-of-sight path following of underactuated marine craft. *Proceedings of the 6th IFAC MCMC, Girona, Spain*, 244–249.

Garau, B., Alvarez, A., and Oliver, G. (2005). Path planning of autonomous underwater vehicles in current fields with complex spatial variability: an a* approach. In *Robotics and Automation, 2005. ICRA 2005. Proceedings of the 2005 IEEE International Conference on*, 194–198. doi: 10.1109/ROBOT.2005.1570118.

Hart, P., Nilsson, N., and Raphael, B. (1968). A formal basis for the heuristic determination of minimum cost paths. *Systems Science and Cybernetics, IEEE Transactions on*, 4(2), 100–107. doi: 10.1109/TSSC.1968.300136.

Mahajan, A. and Walworth, M. (2001). 3d position sensing using the differences in the time-of-flights from a wave source to various receivers. *Robotics and Automation, IEEE Transactions on*, 17(1), 91–94.

Premebida, C. and Nunes, U. (2005). Segmentation and geometric primitives extraction from 2d laser range data for mobile robot applications. *Robotica*, 2005, 17–25.

Zhang, Q. and Pless, R. (2004). Extrinsic calibration of a camera and laser range finder (improves camera calibration). In *Intelligent Robots and Systems, 2004.(IROS 2004). Proceedings. 2004 IEEE/RSJ International Conference on*, volume 3, 2301–2306. IEEE.